Applied Acoustics 103 (2016) 157–162

Contents lists available at ScienceDirect

Applied Acoustics

journal homepage: www.elsevier.com/locate/apacoust

3D FEM analyses of the ultrasonic transducer for controlled nanowire rotary driving

Xiaofei Wang, Junhui Hu *

State Key Lab of Mechanics and Control of Mechanical Structures, Nanjing University of Aeronautics and Astronautics, Nanjing 210016, China

ARTICLE INFO

Article history:
Received 27 December 2014
Received in revised form 26 May 2015
Accepted 3 June 2015
Available online 25 June 2015

Keywords:
NW rotary driving
FEM
Ultrasonic transducer
Vibration

ABSTRACT

Controlled rotary driving of single nano objects is an important technology in the assembling of nano structures, handling of biological samples, nano measurement, etc. However, there have been little analyses on the ultrasonic transducers for the nano rotary driving, which makes the transducer's optimization impossible. In this work, vibration characteristics of the ultrasonic transducer for rotary driving of single nanowires, which has been proposed by the authors' group, are analyzed by the 3D finite element method (FEM), and some useful guidelines for designing the transducer are achieved. It is found that the working point still exists when the commonly used metal materials in ultrasonic transducers are used as the vibration transmission strip, and when the vibration transmission strip's size changes. It is also found that the direction of the elliptical motion of the micro manipulating probe's tip may be reversed by changing the size of the vibration transmission strip properly. In addition, to ensure the performance consistency of the device, the micro manipulating probe's length L_m or driving frequency should be designed to avoid the resonance of the micro manipulating probe.

1. Introduction

Controlled rotary driving of nano entities is useful in the assembling of nano structures, orientation of samples in bioengineering, and measurement of nano materials [1]. Major physical principles, tried to rotary drive nanoscale entities, include laser beams [2,3], electromagnetic fields [4,5], and ultrasound [6–9]. Of all the methods, the ultrasonic rotary driving has the merits such as no selectivity to manipulated objects, no heat damage to biological samples (for some principles), simple and compact structure, and light weight. In 2012 and 2014, our research group reported the methods to rotate the silver nanowires by acoustic streaming in water film on an ultrasonic stage [7], and to rotate a single silver nanowire by acoustic streaming eddies around a micro manipulating probe (MMP) [8], respectively. Similar working principle was also reported by another research group in 2014 [9], to rotary drive single gold nano rods. However, there have been little analyses on the ultrasonic transducers employed in the rotary driving of the two researches.

In this work, vibration characteristics of the ultrasonic transducer with a MMP for nanowire (NW) rotary driving are analyzed by the finite element method (FEM). The computational results can well explain the previously reported phenomenon of NW rotary driving. Useful guidelines for designing the transducer and the MMP are achieved.

2. Ultrasonic transducer for the NW rotary driving

The experiments are conducted under an optical microscopy (VHX-1000E, Keyence), as shown in Fig. 1. In the experiments, a MMP which is mechanically excited to vibrate by a perpendicular vibration transmission strip is immersed into a water film of NW suspension on a silicon substrate. The MMP has a uniform diameter of 10 μm and total length of 3.2 mm. The vibration excitation section of the MMP is 2 mm, which is bonded onto the vibration transmission strip. The suspension is composed of deionized water and dispersed AgNWs which have a diameter of about 100 nm and length of several micrometers to several ten micrometers. The distance between the MMP and silicon substrate is about 10 μm.

Fig. 2 shows the structure and size of the vibration excitation system. The vibration transmission strip made of copper is bonded onto the side of one of the two end plates of a sandwich type piezoelectric transducer. A multilayer piezoelectric vibrator consisting of four piezoelectric rings is pressed by the two end plates via a bolt structure. The neighboring piezoelectric rings are aligned with opposite poling directions. The size of each end plate is $20 \times 20 \times 2\ mm^3$, and outer diameter, inner diameter and

* Corresponding author.
E-mail address: ejhhu@nuaa.edu.cn (J. Hu).

http://dx.doi.org/10.1016/j.apacoust.2015.06.002
0003-682X/

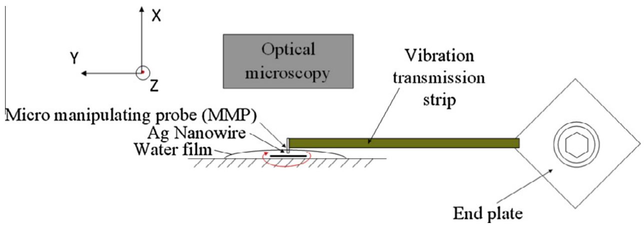

Fig. 1. Experimental setup and the ultrasonic device for the rotary driving of a single AgNW in water film on a silicon substrate.

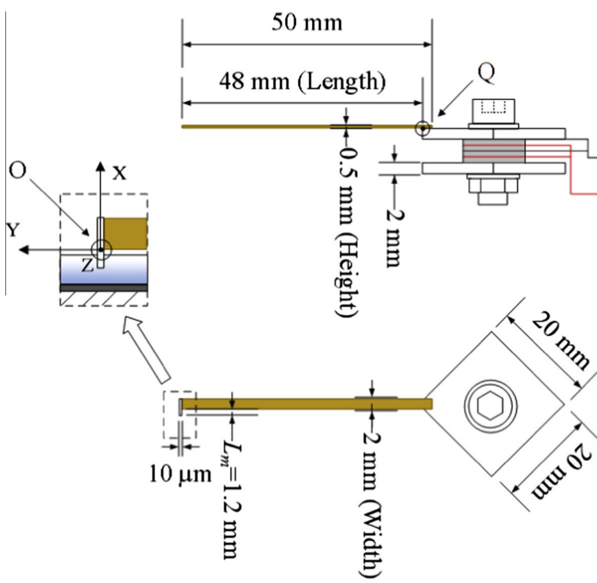

Fig. 2. The structure and size of the vibration excitation system.

thickness of each piezoelectric ring are 12 mm, 6 mm and 1.2 mm, respectively. The piezoelectric constant d_{33} is 250×10^{-12} C/N, electromechanical coupling factor k_{33} is 0.63, mechanical quality factor Q_m is 500, dielectric dissipation factor $\tan\delta$ is 0.6%, and density is 7450 kg/m^3. The two end plates are square. The vibration transmission strip is bonded onto the surface of one of the end plates along the diagonal direction by adhesive material.

If an AgNW lying on the substrate surface in a water film is in the working range [8], it can be sucked towards to the MMP, and rotated around its center or one of its two ends under the tip of the MMP.

3. FEM model of the device

The ANSYS software is used in the FEM analyses. Because the size of the MMP is very small compared to those of the vibration transmission strip and transducer, the FEM analyses of the MMP and the rest part of the device are separated for the convenience of computing the effects of the MMP's length and driving frequency on the vibration amplitude of the MMP's tip. Due to the very small size and mass of the MMP, this simplification has little effect on the computational results of the vibration transmission strip and transducer. Fig. 3(a) shows a 3D FEM model of the device without the MMP, and Fig. 3(b) a 3D FEM model of the MMP. The material constants used in the calculation, other than those of the piezoelectric components, are listed in Table 1. And the property constants and dimensions of the piezoelectric components are given in the discussion of Fig. 2. The solid5 elements are used for the ceramics and the solid45 elements elsewhere; the maximum size of mesh is 0.05 mm in the vibration transmission strip and 2 mm elsewhere; a constant damping ratio (0.003) and the full method solver are used for the harmonic response calculation; both of the solid5 and solid45 elements are three dimensional; the solid5 element has 8 nodes with 6° of freedom at each node, which may be used in the FEM analysis of piezoelectric structures; the solid45 element has 8 nodes with 3° of freedom at each node, which may be used in general structures. In the calculation, unless otherwise specified, the driving voltage is sinusoidal with a peak–peak value of 10 V_{p-p}.

Fig. 4(a) shows the computed amplitudes of *X*-, *Y*- and *Z*-directional vibration displacements at point *O* at the MMP's root (see Fig. 2) versus driving frequency at a driving voltage of 10 V_{p-p}. It shows that the resonance frequency of the device is 93 kHz, which agrees with the measured one [8]. Fig. 4(b) shows the computed *Z*-directional vibration mode of the vibration transmission strip-end plate structure at 93 kHz. However, in the experiments, no phenomenon of nanowire rotary driving could be observed at 93 kHz. This can be well explained by the vibration mode shown in Fig. 4(b). From Fig. 4(b), it is seen that the tip of the vibration transmission strip has a non-uniform vibration along the width direction, which means the phase of the *Z*-directional vibration of the MMP's root is not constant. For this reason, the MMP cannot vibrate elliptically, and thus the acoustic streaming eddy around the MMP cannot be generated. Actually working frequency of the device was 137 kHz in the experiments [8], at which a steady nanowire rotary driving could be observed. Thus the device as a whole is not in resonance at the working point. The analyses in the later part of this paper show that at the working frequency, the end plate actually vibrates flexurally.

4. FEM computation results and discussion

The phase of *Y*-directional vibration displacement minus that of *Z*-directional vibration displacement for a point on the vibration transmission strip is defined as $\Delta\varphi$, and its values at point *O* and *Q* (see Fig. 2) are denoted as $\Delta\varphi_O$ and $\Delta\varphi_Q$, respectively. Fig. 5 shows the calculated phase difference $\Delta\varphi_O$ versus driving frequency. The dotted horizontal lines have ±90° phase difference. It is seen that there exist some frequencies at which $\Delta\varphi_O = \pm 90°$, which means that the resultant of the *Y*- and *Z*-directional vibration components of the MMP is an elliptical motion. Thus at these driving frequencies, eddies can be generated around the MMP, which can drive the NWs to rotate. This well explains the experimental phenomenon reported in our previous work [8]. Moreover, based on the order of magnitude of measured and computed vibration displacement at point *O*, it is known that driving point *A* in Fig. 5 corresponds to the working point in the experiments. The measured vibration displacement components $U_{O,y}$ and $U_{O,Z}$ at point *O* are 97 nm and 42 nm respectively, at 10 V_{p-p}. And the calculated vibration displacement components $U_{O,y}$ and $U_{O,Z}$ at point *O* are 68 nm and 17 nm, respectively, at the same driving voltage. At other driving frequencies with $\Delta\varphi_O$ of ±90°, the computed order of magnitude of vibration displacement at point *O* is less or greater than several ten nanometers. The frequency of driving point *A* in Fig. 5 is 128.2 kHz, and working frequency in the experiments is around 137 kHz. The difference between them could be caused by the errors in the material property constants and the neglect of the adhesive point.

Fig. 6(a) shows the computed out-of-plane vibration mode of one of the end plates at 128.2 kHz. It is seen that the maximum vibration displacement occurs at the corner. This is why when the vibration transmission strip is bonded onto the corners of one of the end plates, mechanical excitation for the vibration transmission strip is most effective. Also, as the vibration transmission